

Modelling of Permanent Magnet Synchronous Motor Incorporating Core-loss

K. Suthamno and S. Sujitjorn

Control and Automation Research Unit, Power Electronics, Machines and Control
Research Group, School of Electrical Engineering, Suranaree University of Technology,
Nakhon Ratchasima, 30000, Thailand

Abstract: This study proposes a dq-axis modelling of a Permanent Magnet Synchronous Motor (PMSM) with copper-loss and core-loss taken into account. The proposed models can be applied to PMSM control and drive with loss minimization in simultaneous consideration. The study presents simulation results of direct drive of a PMSM under no-load and loaded conditions using the proposed models with MATLAB codes. Comparisons of the results are made among those obtained from using PSIM and SIMULINK software packages. The comparison results indicate very good agreement.

Key words: Dq-axis, losses, modelling, permanent magnet synchronous motor

INTRODUCTION

Present-day industry has widely utilized Permanent Magnet Synchronous Motors (PMSM) because of their several advantages. These include high efficiency, low maintenance, high power-factor and ruggedness. Some applications, such as hybrid vehicles, aircrafts, automated machines etc., usually require accurate control of speed and position. Control difficulty arises since a PMSM has complex dynamic that results in complicated modelling. In classical machine textbooks, readers often find equivalent circuit, phasor and differential equation models, for instance books authored by Fransua and Magureanu (1984) and Ong, (1998). DQ-axis models, or dq-models, of PMSMs are also available (Pillay and Krishnan, 1989; Monajemy and Krishnan, 2001; Krishnan, 2010). The dq-models are useful for machine control in the sense that relevant ac-signals are presented as dc-signals. To achieve minimum loss drive of a PMSM, its models with core-loss taken into account is desired. Equivalent circuit models for the purpose are available (Morimoto *et al.*, 1994; Fernandez-bernal *et al.*, 2011; Cavallaro *et al.*, 2005; Lin *et al.*, 2009). The equivalent circuit models provide an insight for loss minimization, however cannot provide accurate dynamic performances of the machines. In contrast, the dq-models provide accurate information concerning machine dynamic and control. However, the available dq-models do not incorporate loss terms. Use of the models is thus limited to machine control and drive without an extension to cover loss minimization.

This study proposes the dq-models of PMSMs that incorporate core-loss as well as the equivalent circuit

models. The proposed models are applied to simulations using MATLABTM. The results are compared with those of commercial software packages including PSIMTM and SIMULINKTM with PowerSim Blockset.

MATERIALS AND METHODS

Modelling of a PMSM herein considers both copper- and core-losses designated as R_s and R_c , respectively. Figure 1 illustrates the diagram representing a PMSM, the symbols in which are listed by the end of the study. $v_{Sabc} = [v_{sa} \ v_{sb} \ v_{sc}]^T$ and $i_{Sabc} = [i_{sa} \ i_{sb} \ i_{sc}]^T$ are the voltage and the current vectors, respectively, at the motor terminals. The voltage and the current vectors at the motor cores are represented by $v_{sabc} = [v_{ca} \ v_{cb} \ v_{cc}]^T$ and $i_{cabc} = [i_{ca} \ i_{cb} \ i_{cc}]^T$, respectively. $i_{oabc} = [i_{oa} \ i_{ob} \ i_{oc}]^T$ is the rotor current vector. The following matrices designate the inductances and flux:

$$L_{msabc} = \begin{bmatrix} L_0 - L_{ms} \cos 2(\theta_{re}) - \frac{1}{2} L_o - L_{ms} \cos 2\left(\theta_{re} - \frac{\pi}{3}\right) \\ -\frac{1}{2} L_o - L_{ms} \cos 2\left(\theta_{re} + \frac{\pi}{3}\right) \\ -\frac{1}{2} L_o L_{ms} \cos 2\left(\theta_{re} - \frac{\pi}{3}\right) L_0 - L_{ms} \cos 2\left(\theta_{re} - \frac{2\pi}{3}\right) \\ -\frac{1}{2} L_o - L_{ms} \cos 2(\theta_{re} - \pi) \\ -\frac{1}{2} L_o - L_{ms} \cos 2\left(\theta_{re} + \frac{\pi}{3}\right) - \frac{1}{2} L_o - L_{ms} \cos 2(\theta_{re} + \pi) \\ L_0 - L_{ms} \cos 2\left(\theta_{re} + \frac{2\pi}{3}\right) \end{bmatrix} \quad (1)$$

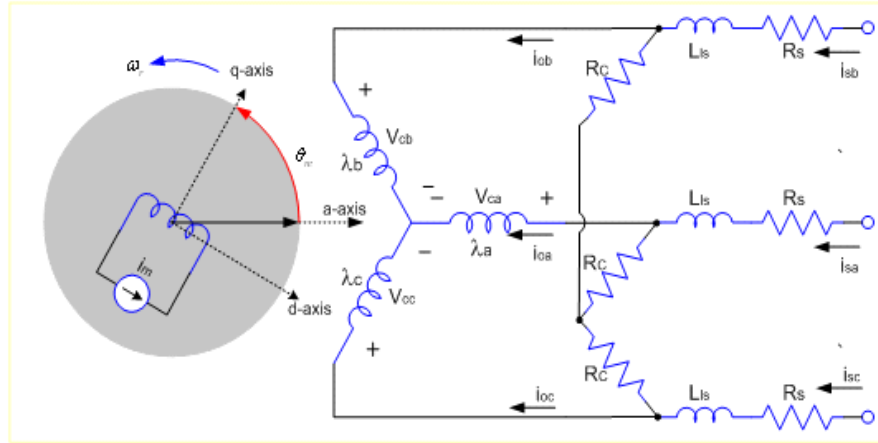


Fig. 1: Diagram representing a PMSM

$$L_{ls} = \begin{bmatrix} L_{ls} & 0 & 0 \\ 0 & L_{ls} & 0 \\ 0 & 0 & L_{ls} \end{bmatrix} \quad (2)$$

$$\Lambda_{PMabc} = \begin{bmatrix} \lambda_{PM} \sin(\theta_{re}) \\ \lambda_{PM} \sin\left(\theta_{re} - \frac{2\pi}{3}\right) \\ \lambda_{PM} \sin\left(\theta_{re} + \frac{2\pi}{3}\right) \end{bmatrix} \quad (3)$$

$R_s = \text{diag}[R_s R_s R_s]$ and $R_c = \text{diag}[R_c R_c R_c]$ represent the winding and the core resistances, respectively. Therefore, Eq. (4) expresses the motor voltage:

$$v_{Sabc} = R_s i_{Sabc} L_{ls} + \frac{d}{dt} i_{Sabc} + v_{Cabc} \quad (4)$$

and Eq. (5) expresses the voltage across the motor cores:

$$v_{Cabc} = \frac{d}{dt} \Lambda_{abc} \text{ or } R_c i_{Cabc} \quad (5)$$

Let $v_{s_{qdo}} = [v_{sq} \ v_{sd} \ v_{s0}]$, $i_{s_{qdo}} = [i_{sq} \ i_{sd} \ i_{s0}]$

and $\Lambda_{qdo} = [\lambda_q \ \lambda_d \ \lambda_0]^T$ be the terminal voltages, currents and magnetic flux in dq0-frame, respectively. Transformation from the three-phase abc-frame to the dq0-frame utilizes the transformation matrix:

$$T_{qdo}(\theta_{re}) = \frac{2}{3} \begin{bmatrix} \cos(\theta_{re}) & \cos\left(\theta_{re} - \frac{2\pi}{3}\right) & \cos\left(\theta_{re} + \frac{2\pi}{3}\right) \\ \sin(\theta_{re}) & \sin\left(\theta_{re} - \frac{2\pi}{3}\right) & \sin\left(\theta_{re} + \frac{2\pi}{3}\right) \\ \frac{1}{2} & \frac{1}{2} & \frac{1}{2} \end{bmatrix} \quad (6)$$

Therefore, we can state that $v_{s_{qdo}} = T_{qdo}(\theta_{re}) v_{s_{abc}}$ and $v_{s_{abc}} = T_{qdo}^{-1}(\theta_{re}) v_{s_{qdo}}$, where (θ_{re}) stands for an electrical reference angle of the rotor shaft. Since:

$$v_{s_{qdo}} = R_s i_{s_{qdo}} + L_{ls} \frac{d}{dt} i_{s_{qdo}} + v_{C_{qdo}} + \omega_{re} L_{ls} \begin{bmatrix} 0 & 1 & 0 \\ -1 & 0 & 0 \\ 0 & 0 & 0 \end{bmatrix} i_{s_{qdo}} \quad (7)$$

the rate of change of the motor current wrt time in dq0-frame can be expressed as:

$$\frac{d}{dt} i_{sq} = \frac{1}{L_{ls}} (v_{sq} - (R_s + R_c) i_{sq} + R_c i_{oq} - \omega_{re} L_{ls} i_{sd}) \quad (8)$$

$$\frac{d}{dt} i_{sd} = \frac{1}{L_{ls}} (v_{sd} - (R_s + R_c) i_{sd} + R_c i_{od} + \omega_{re} L_{ls} i_{sq}) \quad (9)$$

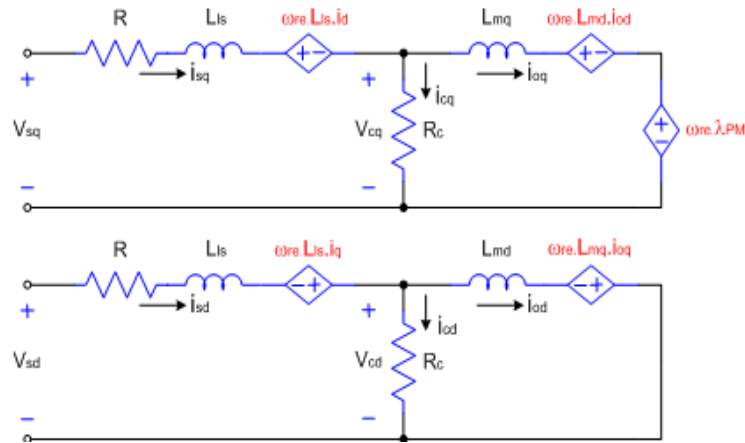
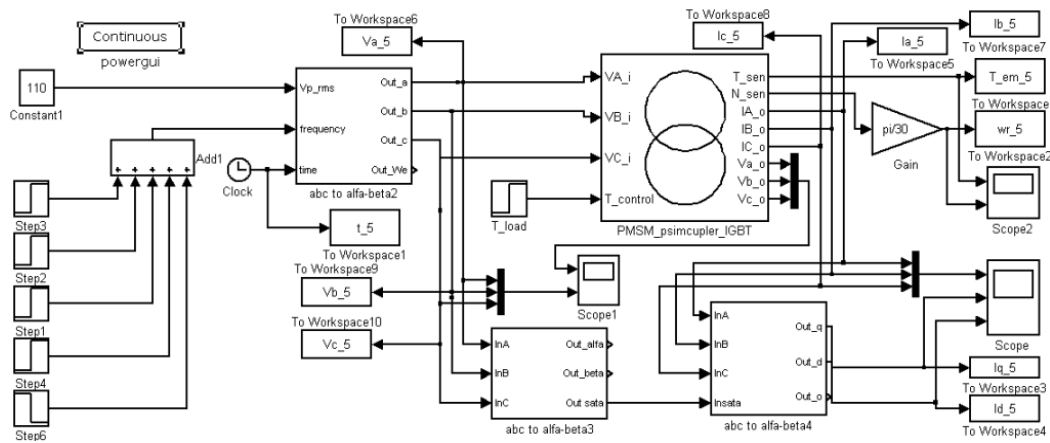
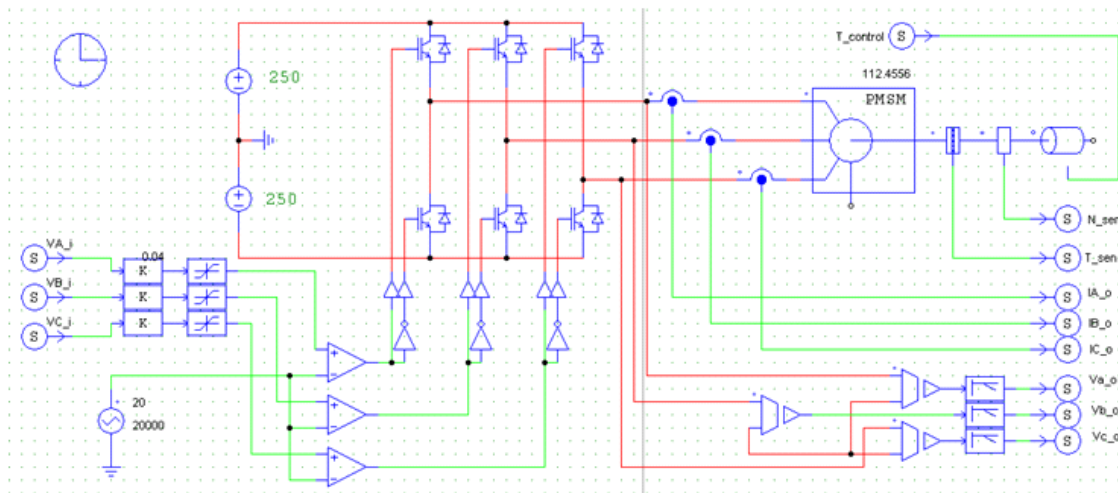


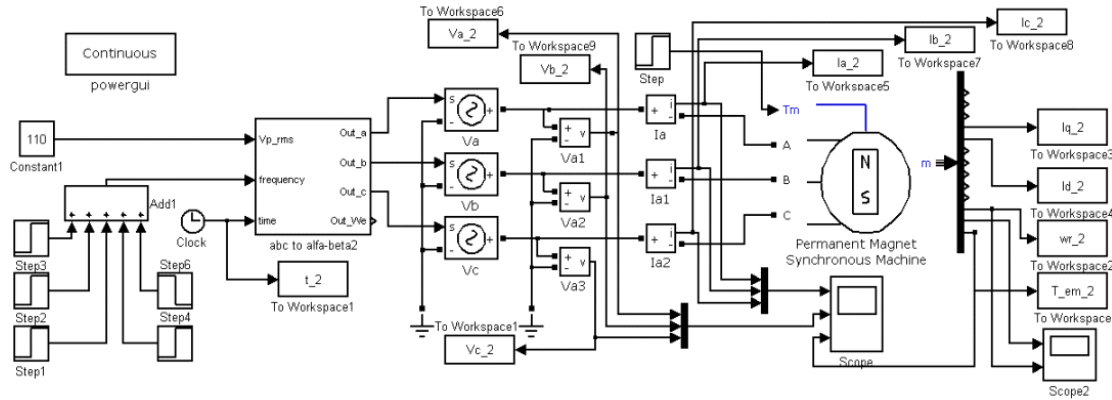
Fig. 2: Equivalent circuits of a PMSM taking account of core-loss and separated inductances



(a)



(b)



(c)

Fig. 3: Simulation diagrams, (a) PSIM, (b) internal simulation diagram of the PMSM coupler module in (a), (c) SIMULINK with PowerSim Blockset

Table 1: Parameters of a PMSM for simulations

Parameters	Proposed mode	SIMULINK	PSIM
R_s (Ω)	1.9	1.9	1.9
R_c (Ω)	330	NA	NA
L_{ls} (mH)	0.77	NA	NA
L_{md} (mH)	15.75	NA	NA
L_{mq} (mH)	31.05	NA	NA
L_{qd} (mH)	NA	16.52	16.52
L_{cq} (mH)	NA	31.82	31.82
λ_{PM}	0.31*	0.31*	112.45**
J ($\text{kg}\cdot\text{m}^2$)	0.0005	0.0005	0.0005
B ($\text{Nm}\cdot\text{s} / \text{rad}$)	0.03	0.03	0.03

*:in V. s / rad; **:in $V_{\text{peak } L-L} / \text{Krpm}$

$$\frac{d}{dt} i_{so} = \frac{1}{L_{ls}} (v_{so} - R_s i_{so}) \quad (10)$$

Since

$$v_{C_{qdo}} = \frac{d}{dt} \Lambda_{qdo} + \omega_{re} M \Lambda_{qdo} \quad (11)$$

and

$$\Lambda_{dgo} = \begin{bmatrix} L_{mq} & 0 & 0 \\ 0 & L_{md} & 0 \\ 0 & 0 & 0 \end{bmatrix} \begin{bmatrix} i_{oq} \\ i_{od} \\ i_{o0} \end{bmatrix} \begin{bmatrix} 0 \\ \lambda_{PM} \\ 0 \end{bmatrix} \quad (12)$$

one can obtain that:

$$\frac{d}{dt} \Lambda_{qdo} = R_c (i_{sqdo} - i_{oqdo}) - \omega_{re} M \Lambda_{qdo} \quad (13)$$

Hence, the rate of change of the torque generating currents in dq-frame wrt time can be expressed as:

$$\frac{d}{dt} i_{oq} = \frac{1}{L_{mq}} \begin{pmatrix} R_c i_{sq} - R_c i_{oq} \\ -\omega_{re} L_{md} i_{od} - \omega_{re} \lambda_{PM} \end{pmatrix} \quad (14)$$

$$\frac{d}{dt} i_{od} = \frac{1}{L_{md}} (R_c i_{sd} - R_c i_{od} + \omega_{re} L_{mq} i_{oq}) \quad (15)$$

Based on the derived voltage and current equations, the equivalent circuits as shown in Fig. 2 can be obtained. Eq. (16) to (19) express the input power, output power, electromagnetic torque and the rate of change of speed of the motor, respectively.

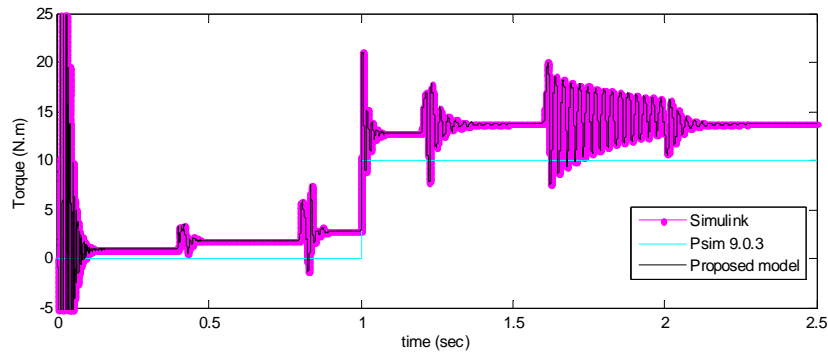
$$P_{in} = \frac{3}{2} (v_{sq} i_{sq} + v_{sd} i_{sd}) = \frac{3}{2} \left(R_s (i_{sq}^2 + i_{sqd}^2) + R_c (i_{cq}^2 + i_{cd}^2) + L_{ls} (i_{sq} l_{sq} + i_{sd} l_{sd}) + L_{mq} i_{sq} l_{sq} + L_{md} l_{sd} i_{sd} \right) + P_{out} \quad (16)$$

$$P_{out} = \frac{3}{2} \omega_{re} (\lambda_{PM} i_{oq} + (L_{md} - L_{mq}) i_{oq} i_{od}) \quad (17)$$

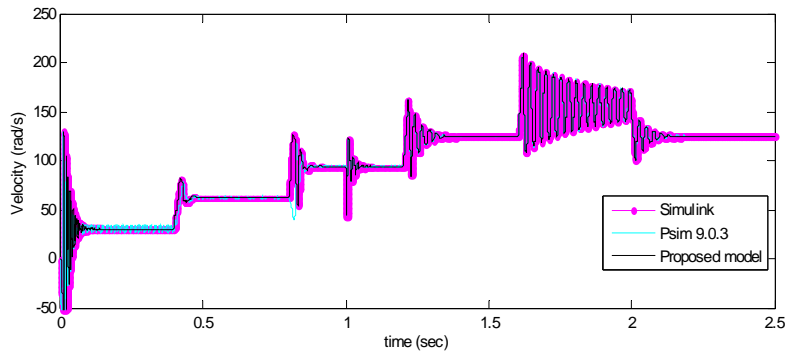
$$\tau_{em} = \frac{3}{2} \left(\frac{P}{2} \right) (\lambda_{PM} i_{oq} + (L_{md} - L_{mq}) i_{oq} i_{od}) \quad (18)$$

$$\dot{\omega}_r = \frac{1}{J} (\tau_{em} - \tau_{load} - B \omega_r) \quad (19)$$

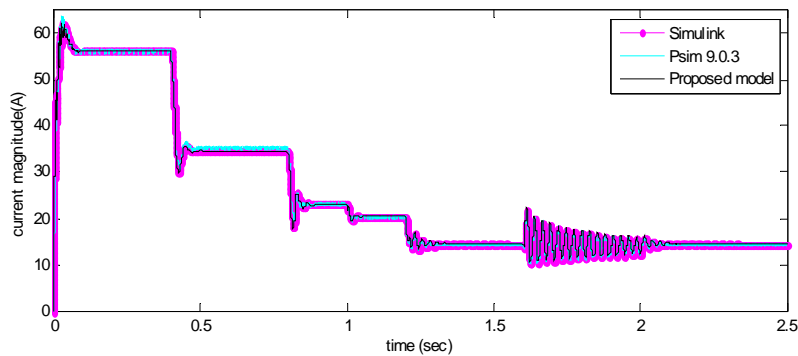
The developed models described so far were coded in MATLAB to simulate the machine dynamic based on a set of parameters (Ong, 1998; Lin *et al.*, 2009) tabulated in Table 1. The results are compared to those obtained from using PSIM and SIMULINK with PowerSim Blockset, respectively. Figure 3 shows the simulation diagrams. In an actual drive, the supply frequency is varied in stepwise manner such that the machine gradually gains its speed. This was conducted accordingly with a frequency-step of 10 Hz in our simulations. For the simulated PMSM, the supply is 110 Vrms, 60 Hz. The



(a)



(b)



(c)

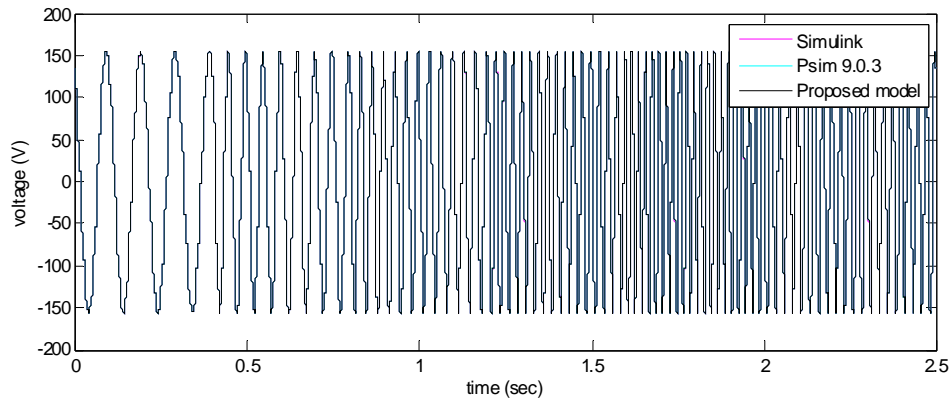
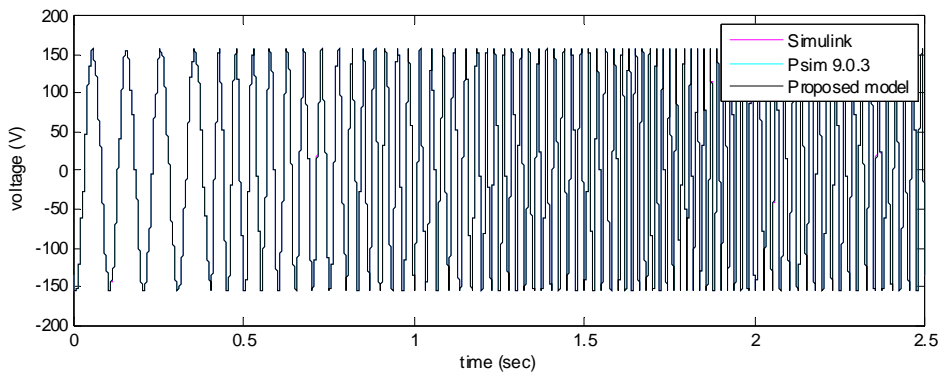
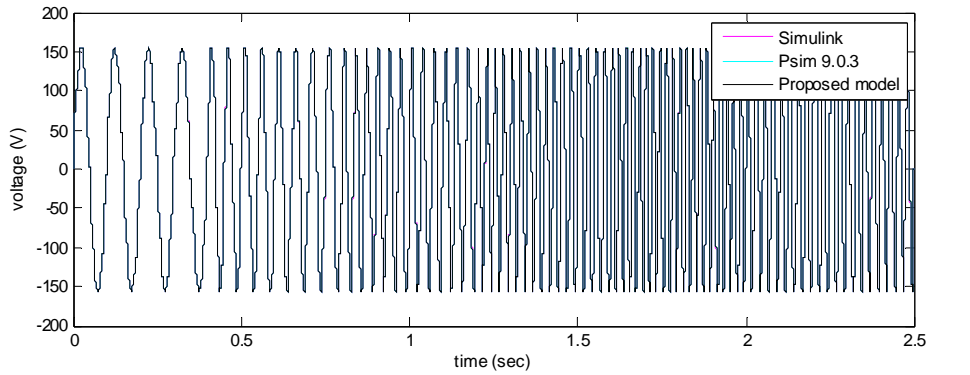
Fig. 4: Motor responses, (a) torque, (b) speed, (c) magnitude of the resultant current

machine was driven at no-load from stand-still up to a speed of 150 rad/s within 1.6-1.7 s. At the moment of 1 s, 10 Nm load was suddenly applied to the machine shaft. At 2 s, the supply frequency was reduced from 50 to 40 Hz.

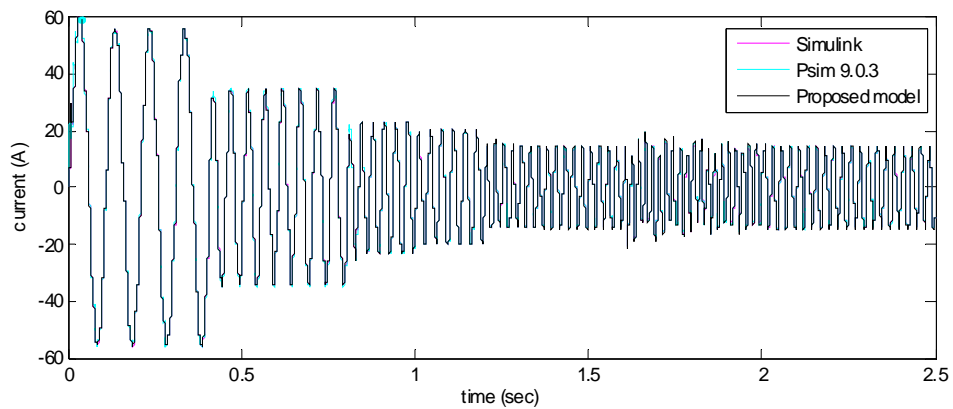
RESULTS AND DISCUSSION

Figure 4 illustrates the simulation results including torque and speed of the motor as well as the magnitude of

the resultant current of the dq-currents. The results obtained from the three simulation approaches agree well except that PSIM gives the mechanical torque at shaft while the other two approaches give the electromagnetic torque. Therefore, the torque curve from PSIM shown in Fig. 4a is lower than the other two curves. The curves indicate oscillatory transient responses at the instant the frequency and the load-torque are changed. Figure 5 shows the motor phase-voltages and -currents. Notice that



(a)



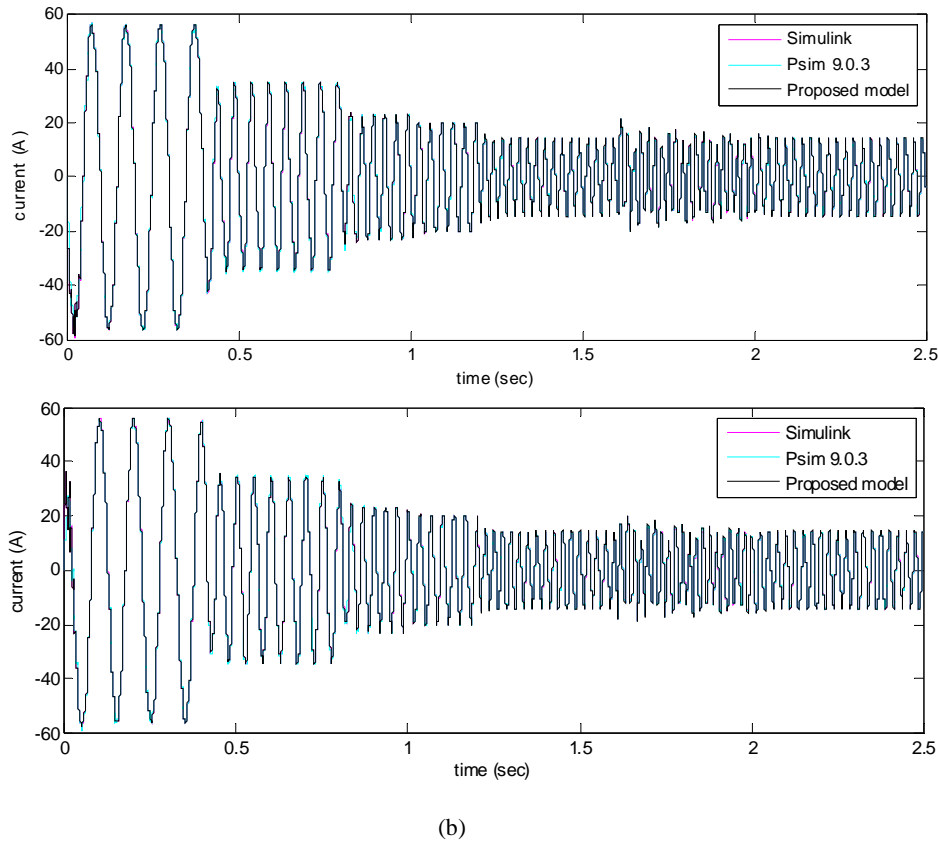


Fig. 5: (a) motor phase-voltages, (b) motor phase-currents (top, middle and bottom windows for phase-a, -b and -c, respectively)

when the motor is driven at 50 Hz, it is almost unstable during which the torque is about rated. The motor can produce a stable rated torque with somewhat lower driving frequency, i.e. 40 Hz, as indicated by the response curves from 2 s onward.

CONCLUSION

This paper has presented the derivation of the dq-axis models of a PMSM with copper- and core-losses under consideration. The proposed models are useful for optimized efficiency drive development of a PMSM. Using MATLAB, PSIM and SIMULINK, simulations of direct-driven machine have been conducted. Comparisons of the results have indicated very good agreement among the three approaches.

NOMENCLATURE

R_s	Stator winding resistance
R_c	Core loss resistance
L_{ls}	Stator leakage inductance
L_0, L_{ms}	Self and mutual inductances
L_{md}, L_{mq}	d- and q-axis mutual inductances
L_d, L_q	d- and q-axis inductances

λ_{PM}	Permanent magnet flux
ω_r, ω_{re}	Mechanical and electrical rotor speeds
τ_{em}	Electromagnetic torque
v_{sd}, v_{sq}	d- and q-axis stator voltages
v_{od}, v_{oq}	d- and q-axis core-loss voltages
i_{sd}, i_{sq}	d- and q-axis stator currents
i_{cd}, i_{cq}	d- and q-axis core-loss currents
i_{od}, i_{oq}	d- and q-axis torque generating currents
P_{in}, P_{out}	Input power and output power
B	Viscous friction coefficient
v_{sabc}, i_{sabc}	Three-phase stator voltage and current vectors
v_{cabc}, i_{cabc}	Three-phase core-loss voltage and current vectors
i_{oabc}	Three-phase torque generating current vectors.
Λ_{abc}	Three-phase stator flux leakage vector
Λ_{qdo}	dq-axis stator flux leakage vector

ACKNOWLEDGMENT

Financial supports from the following organizations are greatly acknowledged: Ministry of Science and Technology (Thailand), Office of Higher Education of Thailand under NRU project and Suranaree University of Technology.

REFERENCES

- Cavallaro, C., A.O. Ditommaso, R. Miceti, G.R. Galluzzo and M. Trapanese, 2005. Efficiency enhancement of permanent-magnet synchronous motor drives by online loss minimization approaches. *IEEE T. Indus. Electr.*, 52: 1153-1160.
- Fernandez-bernal, F., A. Garcia-cerrada and R. Faure, 2001. Determination of parameter in interior permanent magnet synchronous motors with iron losses without torque measurement. *IEEE T. Indus. Appl.*, 37: 1265-1272.
- Fransua, A. and R. Magureanu, 1984. *Electrical Machines and Drive Systems*. Technical Press, Romania.
- Krishnan, R., 2010. *Permanent Magnet Synchronous and Brushless DC Motor Drives*. CRC Press, US.
- Lin, C.K., T.H. Liu and C.H. Lo, 2009. Sensorless interior permanent magnet synchronous motor drive system with a wide adjustable speed range. *IET Electric Power Applications*, 3(2): 133-146.
- Monajemy, R. and R. Krishnan, 2001. Control and dynamics of constant-power-loss-based operation of permanent magnet synchronous motor drive system. *IEEE T. Indus. Electr.*, 48(4): 839-844.
- Morimoto, S., Y. Tong, Y. Takeda and T. Hirasu, 1994. Loss minimization control of permanent magnet synchronous motor drives. *IEEE T. Indus. Electr.*, 41(5): 511-517.
- Ong, C.M., 1998. *Dynamic Simulation of Electric Machinery*. Prentice Hall, US.
- Pillay, P. and R. Krishnan, 1989. Modeling, simulation and analysis of permanent-magnet motor drives, part II: The brushless DC motor drives. *IEEE T. Indus. Appl.*, 25(2): 274-279.